Matrix Effects in the Detection of Pb and Ba in Soils Using Laser-Induced Breakdown Spectroscopy

AARON S. EPPLER, DAVID A. CREMERS,* DONALD D. HICKMOTT, MONTY J. FERRIS, and AARON C. KOSKELO

Chemical Science and Technology Division (A.S.E., D.A.C., M.J.F., A.C.K.) and Earth and Environmental Science Division (D.D.H.), Los Alamos National Laboratory, Los Alamos, New Mexico 87545

With the use of laser-induced breakdown spectroscopy (LIBS), the effects of chemical speciation and matrix composition on Pb and Ba measurements have been investigated by using sand and soil matrices. A cylindrical lens was used to focus the laser pulses on the samples because it yielded higher measurement precision than a spherical lens for the experimental conditions used here. The detection limits for Pb and Ba spiked in a sand matrix were 17 and 76 ppm (w/w), respectively. In spiked soil, the detection limits were 57 and 42 ppm (w/w) for Pb and Ba, respectively. Measurement precision for five replicate measurements was typically 10% RSD or less. Two factors were found to influence emissions from Pb and Ba present in sand and soil matrices as crystalline compounds: (1) compound speciation, where Ba emission intensities varied in the order carbonate > oxide > sulfate > chloride > nitrate, and where Pb emission intensities varied in the order oxide > carbonate > chloride > sulfate > nitrate; and (2) the composition of the bulk sample matrix. Emissions from Ba(II) correlated inversely with the plasma electron density, which in turn was dependent upon the percent sand in a sand/soil mixture. The analytical results obtained here show that a field-screening instrument based on LIBS would be useful for the initial screening of soils contaminated with Pb and Ba.

Index Headings: **Laser-induced breakdown spectroscopy; LIBS; Laser microprobe; Atomic emission spectroscopy; Soil analysis.**

INTRODUCTION

Many waste sites nationwide are contaminated with metal pollutants.[1] Extensive efforts are underway to develop remediation programs for these sites, but before remediation efforts begin, sampling plans must be devised that adequately determine the degree of contamination. In many cases, the determination of the areas to be sampled has been based on a combination of professional judgment and site history. In an effort to supplement these assessments, field-portable X-ray fluorescence (XRF) spectrometers have been used to characterize contaminated waste sites.[2,3] Two primary benefits of field-screening instruments, such as a portable XRF unit, are (1) the ability to analyze a large number of samples in a short amount of time, and (2) the low analysis cost per sample (compared with that for a conventional analysis carried out in a laboratory). Disadvantages of field-screening measurements when compared to lab-based analysis are, in general, reduced precision and accuracy and higher detection limits. Even considering these disadvantages, field-screening instruments can be used to (1) define the boundaries of contaminated areas, (2) improve the quality of sampling plans, (3) minimize the number of samples requiring costly and time-consuming conventional analysis, and (4) establish the effectiveness of remediation efforts.

In this paper, we show that laser-induced breakdown spectroscopy (LIBS) is capable of generating semi-quantitative data useful for field-screening operations. In comparison to portable XRF and conventional laboratory-based analytical methods, LIBS offers one or more of the following advantages for field-based soil analysis: (1) simplicity; (2) detection limits and measurement precision sufficient for screening many elements of interest (including but not limited to Be, Cr, Sr, Cd, Ba, and Pb) in soils; (3) rapid sample turnaround times (< 1 min per sample vs. 3–10 min for XRF); and (4) remote analysis capabilities.[4]

A detailed description of the LIBS technique as well as previous applications can be found in several review articles and books;[5–8] four articles discuss soils directly.[9–12] Briefly, the LIBS method uses focused laser pulses to form a microplasma on the surface of the material to be analyzed. Because of the high plasma temperature (6000–9000 K), a small mass of material is vaporized and the resulting atoms are excited to emit light. The spark light is temporally and spectrally resolved, and the emitting species are identified by their unique spectral signatures.

This study reports the effects of analyte speciation and matrix composition on the determination of Pb and Ba in soil and sand with the use of LIBS. These elements were chosen for this work because they are of practical interest to remediation efforts at Los Alamos sites and elsewhere. A thorough understanding of these matrix effects is required to maximize LIBS analytical performance and to determine limitations of the technique for this application.

EXPERIMENTAL

Apparatus. Pulses (10-ns duration) from a Q-switched Nd:YAG laser (Quanta-Ray GCR-3 and DCR-11) operating at the fundamental wavelength (1064 nm) were focused on the sample surface to generate the laser plasmas. The laser pulse repetition rate was 10 Hz unless otherwise noted. Measurements were carried out in air at Los Alamos atmospheric pressure (~580 Torr). The laser pulses were focused on the samples by using either a spherical or a cylindrical lens with a focal length of 150 mm. Unless stated otherwise, the pulse energy incident on the sample was 190 mJ, which gave a power density (calculated at the focal length of the lens) of 15 GW/cm^2 for the spherical lens and 3.2 GW/cm^2 for the cylindrical

Received 10 January 1996; accepted 26 March 1996.
* Author to whom correspondence should be sent.

0003-7028/96/5009-1175$2.00/0

lens. A 2-m-long fused-silica fiber-optic cable, attached to a 0.5-m-focal-length spectrograph (Model 1870, Spex Industries), collected the spark light. Gratings of 3600, 2400, and 1200 lines/mm were used in the spectrograph to adjust the resolution and spectral coverage as needed. The spectrally resolved light was recorded by using a gated, intensified photodiode array (Princeton Instruments, Model ST-120 controller, IRY-1000S/RB detector, or Tracor Northern, Model TN-6500 controller, TN-6132 detector), with ~0.1 nm resolution. The system geometry is similar to that described elsewhere.[13] In this paper, a measurement is defined as the average of spectra from 100 sparks. Repetitive sparking on a stationary particulate sample formed a crater which changed the lens-to-sample distance. Since previous work has demonstrated that changes in the lens-to-sample distance can significantly affect analyte emissions,[9,14] the samples were moved continuously with a motorized translation stage.

In our detection system, the time delay (t_d) is defined as the time elapsed between plasma formation and gating on of the detector intensifier to collect the spark light. The detection window (t_b) is defined as the time span over which the plasma light was recorded. All measurements were taken with the use of t_d = 1 μs and t_b = 50 or 200 μs. Initial experiments were made with t_b = 200 μs, to ensure maximization of the analyte signal from the decaying plasma. Subsequently, it was determined that for times greater than 50 μs the analyte emissions had completely decayed, so that detection windows longer than 50 μs were unnecessary. The delay time of 1 μs was chosen to minimize the intensity of the continuum present early in the lifetime of the plasma. The time delay and detection window were adjusted with a pulse generator (Stanford Research Systems, Model DG 535) synchronized to the laser output pulses.

Analyte signals were determined by measuring the net peak area under the analyte emission lines. In some measurements, the ratio of the analyte signal to the signal from another element in the sample at a fixed concentration (reference element) was computed. Computing the emission signal ratio between elements with similar upper energy levels can minimize changes in the analyte signal caused by small fluctuations in plasma excitation conditions.

Sample Preparation. The matrices used here were sand (98.9% pure sand, Baker, Inc.) and clean Los Alamos soil. Crystalline compounds of Ba, Cr, and/or Pb were added to each matrix to prepare samples having known concentrations of these elements. In this paper, concentrations refer to ppm or percent concentration of analyte mass to total sample mass. Each mixture was ground and homogenized in a tungsten carbide shatterbox for 1 to 9 min (Chemplex Industries, Model S60AAW-6118 Spectromill). Binders typically used for X-ray fluorescence [either X-ray Mix (Spex Industries) or cellulose (FMC Corporation)] were then added at 10% (w/w) to each mixture, and grinding was continued for an additional 1.5 min. Binder was added to the mixture to reduce dust generated during laser sampling and to maintain the integrity of the pressed samples. Finally, a portion of each mixture was transferred into an aluminium dish (30-mm diam. × 7-mm deep) and was compacted into a pellet, with the use of a force of approximately 20 tons for 10 min. In those experiments involving graphite added to soil without binder, the samples were not compacted, because the surface did not remain flat when interrogated by the laser pulses.

TABLE I. Comparison of RSD values obtained by focusing laser pulses using a spherical and a cylindrical lens.[a]

Run	RSD (%)[b]	
	Cylindrical lens	Spherical lens
Ba(II)/Si(I)[c]		
1	2.3	17.0
2	1.9	14.8
3	1.7	15.6
Ba(II)/C(I)[c]		
1	3.3	5.8
2	4.2	6.0
3	2.1	2.0
4	1.3	4.1

[a] The focal lengths of the lenses were 150 mm. The Ba concentration in the samples was 8%.
[b] The RSD values were computed from ten replicate measurements.
[c] The ratios were computed with the Ba(II) 233.5-, Si(I) 243.5-, and C(I) 247.8-nm emission lines.

RESULTS AND DISCUSSION

Measurement Precision and Reproducibility. With the use of a spherical and cylindrical lens (150-mm focal length) to form the laser plasmas on the sample surface, measurements were made to determine which type of lens maximized precision. A spherical lens produced a spark resembling an inverted cone with the apex located on the sample surface (spot diameter ≈ 0.4 mm). A cylindrical lens produced a "long spark" of dimensions 6-mm long × 0.1-mm wide on the sample, thereby sampling an area significantly larger than that sampled by the spherical lens, when the lens-to-sample distance was approximately equal to the lens focal length.[15] The Ba(II) line at 233.5 nm was used for most measurements reported here because useful reference lines, C(I) at 247.8 nm (from the binder) and Si(I) at 243.5 nm (from SiO_2 in the sand and soil), were in the same spectral region. Useful reference lines, either from first- or second-order wavelengths of Si, were not found adjacent to the strong Ba(II) line at 455.4 nm. Spectral coverage with the 1200-lines/mm grating was not great enough to detect both Ba(II) at 455.4 nm and the second-order wavelength of C(I) 247.8 nm.

In a direct comparison of the spherical and cylindrical lenses, the results of 10 replicate measurements of Ba in soil show that the relative standard deviation (RSD) values of the Ba(II)/Si(I) ratio obtained with the spherical lens were higher than those obtained with the cylindrical lens (Table I). In contrast, the RSD values obtained for the Ba(II)/C(I) ratio were nearly identical for the two lenses. These results may be interpreted in terms of sample homogeneity on the scale of the focused laser pulse spot dimensions. Spatially, the reference element, C, appears homogeneous to both lenses, since the C-containing binder is present as a fine powder (particle sizes < 25 μm). This homogeneity is reflected in the low RSD values for Ba(II)/C(I) obtained by using either lens. On the other hand, the Si-containing sand is composed of larger

TABLE II. Reproducibility of LIBS measurements.[a]

	Ba(II)/Si(I) from $BaCO_3$		Ba(II)/Si(I) from BaO	
	Mean[b]	RSD (%)	Mean[b]	RSD (%)
Day 1	0.236 ± 0.006	2.7	0.195 ± 0.013	6.5
Day 2	0.235 ± 0.005	2.3	0.202 ± 0.006	2.8
Day 3	0.223 ± 0.006	2.9	0.182 ± 0.005	2.8
Combined values	0.231 ± 0.009	3.8[c]	0.193 ± 0.008	4.0[c]

[a] Mean and RSD values were computed from ten replicate measurements. The ratios were computed with the Ba(II) 233.5- and Si(I) 243.5-nm emission lines. The Ba concentration was 4000 ppm.
[b] The uncertainty in the mean is one standard deviation of 10 replicate measurements.
[c] The RSD of the average was computed with the use of all 30 measurements from the three days.

TABLE III. Comparison of analyte emission intensities from LIBS measurements of different Pb and Ba species spiked in sand.[a]

Compound	Ba(II)/C(I)[b] (× 10^{-2})	Compound	Pb(I)/Cr(I)[b] (× 10^{-2})
$BaCO_3$	53 ± 2.1	PbO	41 ± 0.6
BaO	52 ± 5.2	$PbCO_3$	34 ± 1.0
$BaSO_4$	46 ± 1.2	$PbCl_2$	34 ± 1.0
$BaCl_2$	41 ± 3.2	$PbSO_4$	23 ± 0.5
$Ba(NO_3)_2$	36 ± 1.3	$Pb(NO_3)_2$	13 ± 1.0

[a] The emissions from Ba(II) 233.5-, Pb(I) 405.7-, Cr(I) 425.4-, and C(I) 247.8-nm lines were used for these measurements. The Ba, Pb, Cr, and C concentrations were constant at 2500 ppm, 1000 ppm, 1000 ppm, and 4.4%, respectively, in the different samples.
[b] These values are averages of five replicate measurements. The uncertainty in the average is one standard deviation of the five replicate measurements.

particles (particle sizes = 100–500 μm), so that this matrix appears less homogeneous over the area ablated by the spherical lens in comparison with the much larger area sampled by the cylindrical lens. The seeming decrease in homogeneity accounts for the higher RSD values of the Ba(II)/Si(I) ratio obtained with the spherical lens. With its larger sampling area, the cylindrical lens apparently minimizes sample inhomogeneity effects, so this lens was used for all other measurements reported in this paper.

One impediment to the use of laser-induced plasmas for quantitative or semi-quantitative analysis has been the poor reproducibility of analytical results.[6] In order to determine measurement reproducibility, we analyzed sand samples spiked with 4000 ppm Ba as either BaO or $BaCO_3$ over three days, keeping all measurement parameters constant. These parameters included the laser pulse energy, the time resolution parameters (t_d, t_b), and the geometry of the focusing and detection optics. The daily averages of the Ba(II)/Si(I) ratio and the RSD values computed from 10 replicate measurements of each sample show high precision (Table II). In addition, the Ba(II)/Si(I) mean and RSD values for all 30 measurements demonstrate that the day-to-day reproducibility can also be very high. The laser pulse energy, measured before and after each set of 20 measurements, varied less than 3% from 190 mJ/pulse. These data demonstrate the reproducibility of LIBS measurements when analysis parameters are held constant and when homogeneous matrices of fixed composition are used.

Effect of Chemical Speciation on Analyte Intensities. To investigate the effect of chemical speciation on analyte emission intensities, we analyzed several different Ba and Pb compounds in sand and soil using LIBS. Chemical speciation influenced emissions from both Ba and Pb spiked at constant concentrations in a sand matrix (Table III). In addition, chemical speciation influenced the slopes of calibration curves prepared with different Pb compounds spiked in both sand and soil matrices (Table IV). The concentrations of the reference elements, C (from the binder) and Cr (added at a concentration of 1000 ppm as Cr_2O_3), were constant in each sample set. These data indicate that analyte speciation can affect calibration curves. Consequently, the accuracy of measurements may be reduced for samples in which the exact speciation is unknown because of the difficulty in preparing an appropriate calibration curve.

Calibration curves were also prepared for the strong Ba and Pb emission lines [Ba(II) 455.4 nm and Pb(I) 405.7 nm] with the use of spiked sand, spiked soil, and Ba- and Pb-contaminated soils collected at sites around Los Alamos. The Ba- and Pb-contaminated soil samples collected on site were analyzed with a laboratory X-ray fluorescence spectrometer (Rigaku 3064). Concentrations ranged from 912 to 8912 ppm for Ba and from 367 to 1045 ppm for Pb. Electron microprobe analysis of the Ba-containing soils revealed that the Ba was present as $BaCO_3$, as $BaSO_4$, and as Ba adsorbed to organic matter.[16] Despite this diverse speciation, LIBS analysis resulted in a good linear correlation (r^2 = 0.95) between the Ba intensity measured with LIBS and the Ba concentration determined by XRF (Fig. 1). Additional Ba calibration curves, determined by spiking soil and sand with $BaCO_3$, are shown in Fig. 2. Because of the absence of an atomic emission signal adjacent to the strong Ba(II) line, which would serve as an internal standard, only the net Ba(II) signal is plotted. Regression analysis of the Ba calibration data shows a somewhat better linear correlation for the spiked samples [(r^2 = 0.98) for soil and (r^2 = 0.96) for sand] than obtained for the site-contaminated samples.

A large number of Pb-contaminated soils from Los Alamos sites were not available for calibration experiments. However, a good correlation (r^2 = 0.99) was found for the three contaminated soil samples analyzed (Fig. 3). The Pb(I) line at 405.7 nm and the Fe(I) line at 406.3 nm were used to compute the emission intensity ratio. The detection limits (C_L) for the different Pb-spiked sand

TABLE IV. Detection limits and slopes of calibration curves for Pb compounds in sand and soil matrices.[a]

	Sand			Soil		
Compound	C_L (ppm)[b]	m (Pb/Cr)[c]	m (Pb area)	C_L (ppm)[b]	m (Pb/Cr)[c]	m (Pb area)
PbO	18	3.7 ± 0.3	2000 ± 150	15	4.0 ± 0.2	1590 ± 60
$PbCO_3$	17	3.1 ± 0.2	1430 ± 60	34	2.5 ± 0.1	1080 ± 70
$PbCl_2$	22	2.8 ± 0.2	920 ± 90	6	1.5 ± 0.2	507 ± 40
$PbSO_4$	72	1.7 ± 0.1	514 ± 10	57	1.2 ± 0.1	400 ± 10

[a] Pb concentrations ranged from 50 to 1000 ppm. The Pb(I) line at 405.7 nm and the Cr(I) line at 425.4 nm were used for these measurements.
[b] The detection limit (C_L) was determined by using $C_L = 3s/m$, where s is the standard deviation of replicate measurements for the least concentrated sample, and m is the slope of the calibration curve.
[c] The slopes of the calibration curves for the Pb(I)/Cr(I) ratio are in units of 10^{-4}. The uncertainty is the standard deviation of the slope.

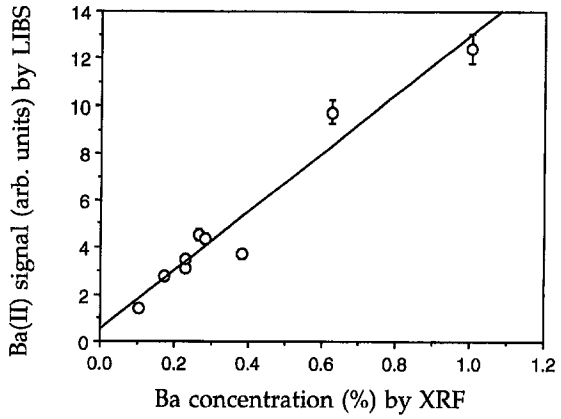

FIG. 1. Relationship between the Ba emission intensity obtained by using LIBS and the Ba soil concentration determined by XRF.

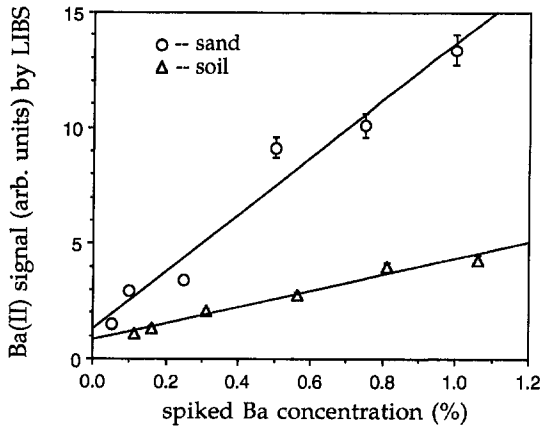

FIG. 2. Calibration curves for $BaCO_3$ powder spiked in sand and soil.

and soil samples are listed in Table IV. Detection limits were determined by using $C_L = 3s/m$, where s is the standard deviation of four measurements of the least concentrated samples, and m is the slope of the linear calibration curve. Although the detection limits are significantly different for some of the Pb-containing compounds, no trend is evident between the two matrices. For comparison, the detection limits for Ba and Pb determined by using the site-contaminated soils and the calibration curves in Figs. 1 and 3 were 63 and 112 ppm, respectively.

The dependence of analyte emission intensities on speciation is not easily explained, but the trends may be related to physical properties of the compounds. For instance, in previous studies of matrix effects, compounds with enthalpies of formation greater than 200 kJ/mol could not be ablated by an unfocused excimer laser.[17] In an attempt to achieve a better understanding of the dependence of analyte signal on chemical speciation, we compared the Pb/Cr and Ba/C ratios from the different compounds with some of the physical properties of the compounds (enthalpy of formation, enthalpy of vaporization, Gibbs enthalpy of formation, entropy, enthalpy of fusion, heat capacity, density, and molar volume). A correlation was deemed significant if the percentage probability that uncorrelated values could achieve the same degree of linear interdependence (based on the number of variables and the quality of the linear regression) was less than 5%.[18]

Molar volume was the only physical property which had a significant correlation with both Pb/Cr and Ba/C ratios from different compounds. It is unclear whether this correlation is anything other than statistically significant. Heat capacities (C_p) and enthalpies of fusion significantly correlated with Ba/C, but not with Pb/Cr. (The linear correlation coefficients, r, for the Ba and Pb correlations with C_p were 0.90 and 0.92, respectively. Although r was slightly better for the Pb data, the heat capacity, known for all five of the Ba compounds, was known only for four of the five Pb compounds, and the reduction of variables lowered the statistical significance of the correlation.) The other properties mentioned, notably including the enthalpy of formation, did not significantly correlate with the Ba or Pb signals from different chemical species. Values for the heat of vaporization (ΔH_{vap}) were found for PbO (207 kcal/mol), $PbCl_2$ (126 kcal/mol), BaO (330.6 kcal/mol), and $BaCl_2$ (246.4 kcal/mol).[19] With only two values for each data set, a correlation is meaningless. However, it is interesting to note that higher ΔH_{vap} values are associated with more intense analyte emissions. This result contradicts the expected relationship between ΔH_{vap} and emission intensity, namely, that ΔH_{vap} will be inversely correlated with emission intensity. Given the variability in the correlations, it is likely that no single physical property of a compound dominates its emission behavior.

Aside from the intrinsic physical properties of the compounds, plasma excitation conditions could be different for each chemical species and correlate with the differences in analyte emissions. For example, Leis and coworkers found plasma temperatures to be significantly different for a range of binary Fe/Cr metals.[20] In this study, the temperatures and electron densities of the plasmas formed on the different samples (containing the different Ba and Pb compounds in sand and soil) were determined by using emissions from five neutral and five singly ionized Ti lines to prepare a Saha–Boltzman plot.[21] Ti was a natural component of both the sand and soil matrices. The analysis conditions for the density and temperature measurements were identical to those used to measure the Ba and Pb emissions from the different compounds. Because the plasma light was collected with a fiber-optic cable, the temperature and electron densities

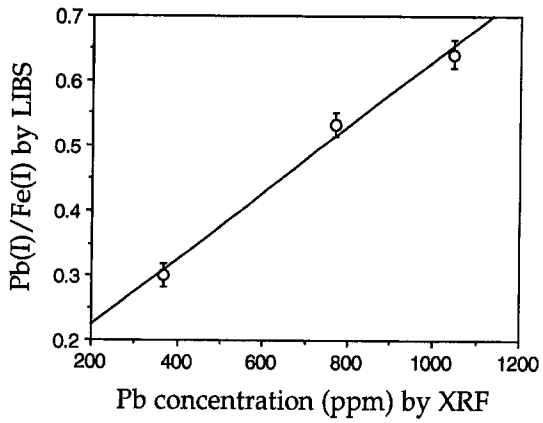

FIG. 3. Relationship between the Pb(I)/Fe(I) ratio obtained by using LIBS and the Pb soil concentration determined by XRF.

were averaged over the plasma volume. The time-averaged (t_d = 1 μs, t_b = 200 μs) temperatures ranged from 4700 to 4800 K (standard deviation = 100 K) among the different compounds, whereas the electron densities ranged from 4.7×10^{16} to 5.3×10^{16} cm^{-3} (standard deviation = 0.2×10^{16}). Because of the long period over which the plasma light was integrated, these average temperatures are lower than those measured soon after plasma formation (6500 K, with t_d = 0.2 μs and t_b = 1 μs). Within the usual accuracy of the electron density and temperature measurements (±10%)[22] and the stated measurement precision, the excitation conditions are considered to be constant for all compounds investigated.

Although neither the plasma temperature nor electron density correlated with the differences in speciation-related emission intensities, the mass of analyte ablated into the plasma will directly affect the analyte emission,[23] and this phenomenon may account for the observed differences in analyte signals. A direct measurement of the crater produced by ablation could not be made for soil samples, because of their particulate nature. Determination of the mass ablated from a soil or sand sample is not possible by measuring mass differences before and after ablation, because of the bulk removal of particles by the pressure/shock waves generated by the laser spark. Instead, we measured the absorptivity of each pure compound, expecting that the emission signal might directly correlate with compound absorptivity. The absorptivities were determined by using low-energy (10 mJ), unfocused laser pulses incident on the pressed compounds. These pulses did not produce a plasma at the surface. An integrating sphere was placed above the samples, and the laser energy reflected from the sample was measured with a high-speed photodiode. At the pulse energy used, the photodiode response to the reflected light was linear. The compound absorptivities were not different within the measurement precision (4%) and thus did not correlate with their respective LIBS emission intensities from the Ba and Pb compounds. These results show that, at low analyte concentrations, the absorptivity of compounds does not account for the compound-dependent Ba and Pb emission intensities observed here.

Effect of Matrix Composition on Analyte Emissions. To determine the effects of the bulk matrix on analyte emission intensities, we used both sand and soil matrices for the calibration experiments. Three important differences between the sand and soil matrices used here are as follows: (1) the absorptivity of pure soil is twice that of pure sand at 1064 nm; (2) after equivalent grinding times, the soil consists of smaller particles than the sand; and (3) the soil contains several elements at significant concentrations having lower ionization potentials than Si and O, the principal elements in the sand (Table V). Although all calibration curves showed a linear dependence of the analyte signal on the analyte concentration, the slopes obtained in the sand and soil matrices were significantly different. For the strong Ba(II) emission at 455.4 nm, the slope of the calibration curve for the sand matrix was greater (by a factor of 3) than the slope for the soil matrix (Fig. 2). Differences in the slopes of calibration curves for Pb in the sand and soil matrices were also observed, although the effect was less significant (Table IV). The exact origin of these differences has not been determined, although some potential causes were explored and these are discussed below.

TABLE V. Main elemental constituents of sand and soil measured with a laboratory-based XRF spectrometer.[a]

Element	Composition (%)		Ionization potential (eV)
	Sand	Soil	
Si	46.2	34.4	8.15
O	52.3	48.1	13.61
Ti	...[b]	0.20	6.82
Al	...[b]	7.24	5.99
Fe	...[b]	2.00	7.87
Na	...[b]	2.42	5.14
K	...[b]	3.32	4.34

[a] Measured by using a Rigaku 3064 XRF spectrometer.
[b] The concentrations of these elements in sand were below the detection limits of the XRF spectrometer.

First, the influence of aerosol formation on emission intensities was investigated. In an effort to explain the different emission intensities of analytes in sand and soil, Wisbrun et al. proposed that an aerosol, which affected the analyte signals, was formed above each sample by the laser pulses focused on the sample surface.[9,11] They found that aerosol production was dependent on the laser repetition rate and that, at 10 Hz, analyte emissions from sand were greater than those from soil, which is consistent with our observation of greater slopes for the sand matrices. We investigated the effect of repetition rate on emission intensities because, on the basis of this prior work, it may account for the slope differences we observed. For all our measurements, the laser pulse energy was held constant. As shown in Fig. 4a, the intensities of Pb(I) at 405.7 nm and Fe(I) at 406.3 nm in soil increased as the repetition rate was increased. The Pb(I)/Fe(I) ratio, however, remained relatively constant as the repetition rate changed (Fig. 4b). In our measurements, although changes in the repetition rate may have changed the aerosol density above the sample, these changes were effectively eliminated by using the Pb(I)/Fe(I) ratio. Therefore, differences in aerosol production above the sand and soil samples cannot account for the different slopes obtained here, since our data show that calibrations with both ratioed and net analyte signals exhibit a dependence on matrix composition.

Another parameter which may influence analyte emissions from sand and soil is matrix absorptivity, as opposed to the compound absorptivity discussed above. In an investigation of this effect, 2500-ppm Ba as $BaCO_3$ was spiked into two sand mixtures, one containing cellulose (10%) and one containing graphite (10%), which absorbed four times as much laser light as the cellulose mixture. Samples used in this experiment were not compacted, since the pressed graphite sample did not remain intact during analysis. To reduce dust and maintain sample integrity, we set the laser repetition rate at 1 Hz, and 30 spectra were averaged to obtain one measurement. When analyzed by LIBS, the net analyte emission intensities from the graphite/sand matrix were twice as intense as those from the cellulose/sand matrix, possibly because of the increased coupling of the laser energy with the graphite powder. However, the Ba(II)/Si(I) ratio was constant for each matrix, indicating that relative emission intensities remained unaffected by the absorptivity of the

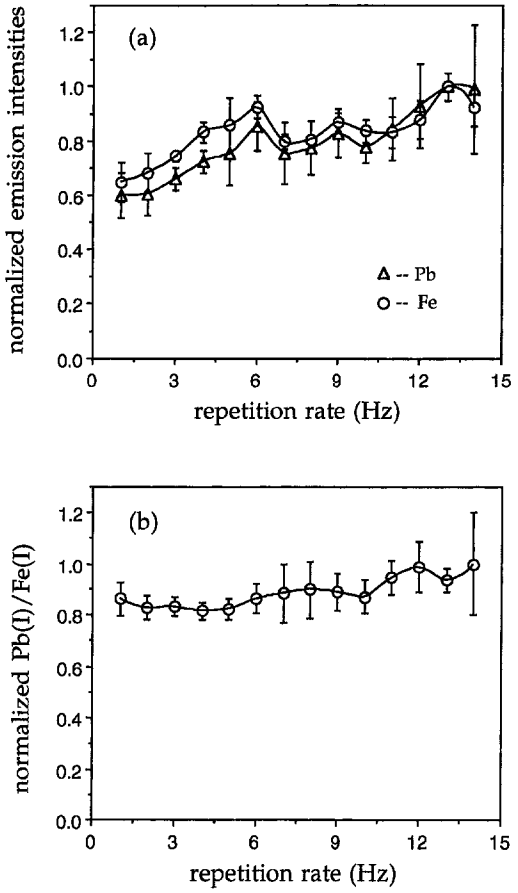

FIG. 4. Effect of laser pulse repetition rate on (**a**) the Pb and Fe emission intensities and (**b**) the Pb(I)/Fe(I) ratio.

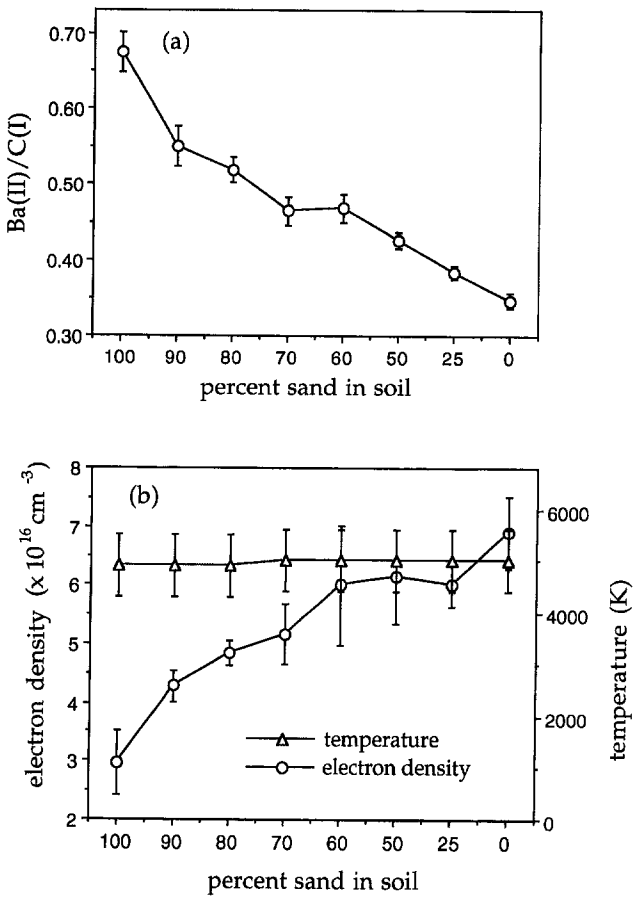

FIG. 5. Dependence of (**a**) the Ba(II)/C(I) ratio and (**b**) the electron density and temperature of the plasma on the composition of a sand/soil matrix.

sample. These results suggest that matrix absorptivity uniformly affects the emission behavior of all elements in the sample and that the relative emission intensities from different elements do not change. Therefore, ratioing two emissions should allow data comparison between samples which have different absorptivities.

In contrast to the results obtained with the cellulose/sand and graphite/sand matrices, the Ba(II) 233.5-nm/C(I) 247.8-nm ratio was found to decrease as the concentration of sand added to a soil matrix decreased (Fig. 5a). Carbon in the binder was used as the reference element because the concentration of this species was constant in these sand and soil mixtures. The several differences between the sand and soil matrices complicated the interpretation of these data; however, some significant relationships were found. Among the differences between the sand/soil matrices, neither absorptivity nor particle size was considered significant, because, as discussed above, computing the Ba(II)/C(I) ratio will minimize absorption effects and the use of the cylindrical lens will minimize inhomogeneity due to particle size. If neither absorptivity nor particle size affects the Ba(II)/C(I) ratio, the elemental composition of the matrix, which changes significantly from the sand to soil, may be largely responsible for the observed differences in analyte emissions from the sand/soil matrices.

To examine this supposition in more detail, we investigated the plasma excitation conditions for each of the sand/soil matrices by determining the temperature and electron density of the plasmas formed on these samples. The electron density was found to increase monotonically from $3.0 \pm 0.6 \times 10^{16}$ cm^{-3} for pure sand to $6.9 \pm 0.7 \times 10^{16}$ cm^{-3} for pure soil as the percent sand in soil ranged from 100% to 0%. The plasma temperature (5000 ± 600 K), however, remained constant for all mixtures (Fig. 5b). Elements found at appreciable concentrations in the soil matrix may have produced the increased electron density, since these elements all have lower ionization potentials than Si and O, the major components of the sand matrix (Table V). Comparison of Figs. 5a and 5b shows that the electron density correlates inversely with the Ba(II)/C(I) ratio. The greater electron density of the plasma formed on soil will reduce the concentration of Ba(II) through ion-electron recombination, thereby decreasing the observed emission intensity from Ba(II). This observation is consistent with the relationship between ionized species and electron density predicted by the Saha equation.[24]

Ba(I) emissions did not follow the same trend as Ba(II) emissions, since over the time interval used for Ba detection (t_d = 1 μs, t_b = 50 μs) the average Ba(II) concentration was only a small fraction of the Ba(I) concentration. Previous measurements of the ratio of ion to neutral atom concentrations in a plasma on a solid in a vacuum showed values between 10^{-3} and 10^{-5}.[25] Therefore, Ba(II) should be more susceptible to small fluctuations in plasma conditions, while Ba(I), present at a much higher

concentration, should not. It is important to note that the differences in the slopes of the calibration curves for the different Pb compounds found for the sand and soil matrices (Table IV) cannot be entirely explained by the analysis just described for Ba(II), since Pb(I), a neutral species, showed the same dependence on the sand and soil matrices as observed for Ba(II). Evidently, other mechanisms are operating that affect analyte emission intensities, and these remain to be studied.

CONCLUSION

LIBS can be used to determine Ba and Pb in soils at concentrations useful for soil screening. With detection limits of 42 and 57 ppm, respectively, for Ba and Pb in soil spiked with these elements, LIBS measurements have sufficient sensitivity to detect these elements well below the Los Alamos National Laboratory screening action level (5400 ppm for Ba and 400 ppm for Pb).[26] Calibration curves were linear over two orders of magnitude for both elements, and measurement precision was highest (2.3% RSD) when a cylindrical lens was used. In addition, the combined measurement precision obtained over a three-day period was 4% RSD or less, indicating good reproducibility.

Both Ba(II) and Pb(I) emissions were dependent on analyte speciation, e.g., nitrate or oxide, in the sample. The effects of speciation on emission signals were not correlated with any single physical property or with the absorptivity of the compounds. However, with changes of the bulk matrix from a pure sand to pure soil composition, the Ba(II)/C(I) signal was found to decrease. The decrease in Ba(II)/C(I) is correlated with an increase in plasma electron density, possibly indicating significant changes in the concentration of ionized species through perturbation of the electron density. Because of the dependence of analyte emissions on chemical speciation and matrix composition, the accuracy of LIBS measurements can be expected to be degraded when calibrations are not compound- and matrix-specific. However, when LIBS is used in the field for soil screening, where the matrix may not be well characterized, the main interests are the determination of highly contaminated areas and the establishment of remediation boundaries, so that high measurement accuracy is not required.

ACKNOWLEDGMENTS

The support given to A. Eppler by the Los Alamos National Laboratory (LANL) Environmental Restoration Project during this work is appreciated. We also thank Karen Schultz Paige for many useful discussions. This work was done under the auspices of the U.S. Department of Energy (DOE). LANL is operated by the University of California for the DOE.

1. Agency for Toxic Substances and Disease Registry Public Health Service, U.S. Department of Health and Human Services (1994).
2. M. Bernick, P. F. Berry, G. R. Voots, G. Prince, J. B. Ashe, J. Patel, and P. Gupta, "A High Resolution Portable XRF HgI_2 Spectrometer for Field Screening of Hazardous Metal Wastes", in *Advances in X-ray Analysis,* C. S. Barrett, J. V. Gilfrich, T. C. Huang, R. Jenkins, G. L. McCarthy, P. K. Predecki, R. Ryon, and D. K. Smith, Eds. (Plenum Press, New York, 1992), Vol. 35, pp. 1047–1053.
3. S. Piorek, "XRF Technique as a Method of Choice for On-Site Analysis of Soil Contaminants and Waste Material", in *Advances in X-ray Analysis,* C. S. Barrett, J. V. Gilfrich, T. C. Huang, R. Jenkins, and P. K. Predecki, Eds. (Plenum Press, New York, 1990), Vol. 33, pp. 639–645.
4. D. A. Cremers, J. E. Barefield II, and A. C. Koskelo, Appl. Spectrosc. **49,** 857 (1995).
5. S. A. Darke and J. F. Tyson, J. Anal. At. Spectrom. **8,** 145 (1993).
6. V. Majidi and M. R. Joseph, Crit. Rev. in Anal. Chem. **23,** 143 (1992).
7. E. H. Piepmeier, *Analytical Applications of Lasers* (John Wiley and Sons, New York, 1986).
8. *Laser-Induced Plasmas and Applications,* L. J. Radziemski and D. A. Cremers, Eds. (Marcel Dekker, New York, 1989).
9. R. Wisbrun, I. Schechter, R. Niessner, and H. Schröder, SPIE **1716,** 2 (1992).
10. R. Wisbrun, R. Niessner, and H. Schröder, Anal. Methods Instrum. **1,** 1 (1993).
11. R. Wisbrun, I. Schechter, R. Niessner, H. Schröder, and K. L. Kompa, Anal. Chem. **66,** 2964 (1994).
12. K. Y. Yamamoto, D. A. Cremers, M. J. Ferris, and L. E. Foster, Appl. Spectrosc. **50,** 222 (1996).
13. D. A. Cremers, Appl. Spectrosc. **41,** 572 (1987).
14. D. A. Cremers and D. J. Romero, SPIE Remote Sensing **644,** 7 (1986).
15. D. A. Cremers and L. J. Radziemski, Appl. Spectrosc. **39,** 57 (1985).
16. A. S. Eppler, R. Brown, and D. D. Hickmott, unpublished results.
17. D. Franzke, H. Klos, and A. Wokaun, Appl. Spectrosc. **46,** 587 (1992).
18. J. R. Taylor, *Introduction to Error Analysis* (University Science Books, Mill Valley, California, 1982), Appendix C.
19. J. A. Dean, *Lange's Handbook of Chemistry* (McGraw–Hill, New York, 1992), pp. 6.108 and 6.117.
20. F. Leis, W. Sdorra, J. B. Ko, and K. Niemax, Mikrochim. Acta **II,** 185 (1989).
21. C. A. Bye and A. Scheeline, Appl. Spectrosc. **47,** 2022 (1993).
22. H. Griem, *Plasma Spectroscopy* (McGraw–Hill, New York, 1964).
23. K. L. Morton, J. D. Nohe, and B. S. Madsen, Appl. Spectrosc. **27,** 109 (1973).
24. W. Lochte-Holtgreven "Evaluation of Plasma Parameters", in *Plasma Diagnostics,* W. Lochte-Holtgreven, Ed. (North Holland Publishing Company, Amsterdam, 1968), p. 149.
25. L. Moenke-Blankenburg, *Laser Microanalysis,* (John Wiley and Sons, New York, 1989), p. 41.
26. "Installation Work Plan for Environmental Restoration, Rev. 3" (Los Alamos National Laboratory, Nov. 1993), LA-UR-93-3987, Vol. I.